Zeghida Chouaib[1], Guedri Abdelmoumene[1], Belyamna Mohamed Amine[1], M. Hadj Meliani[2], Ljubica Milović[3]*

TRANSIENT TEMPERATURE FIELDS EFFECTS ON MULTI-PASS WELDING IN A BUTT JOINT OF AUSTENITIC PIPING

UTICAJI PRELAZNIH TEMPERATURSKIH POLJA NA VIŠEPROLAZNO ZAVARIVANJE U SUČEONOM SPOJU AUSTENITNIH CEVI

Originalni naučni rad / Original scientific paper
UDK /UDC:

Rad primljen / Paper received: 26.05.2023

Adresa autora / Author's address:
[1)] Infra-Res Laboratory, Department of Mechanical Engineering, University of Souk Ahras, Algeria
[*]email: c.zeghida@univ-soukahras.dz
[2)] LPTPM, Hassiba Benbouali University of Chlef, Algeria
[3)] University of Belgrade, Faculty of Technology and Metallurgy, Belgrade, Serbia

Keywords
- residual stresses
- distortions
- finite element analysis
- austenitic piping

Ključne reči
- zaostali naponi
- deformacije
- analiza konačnim elementima
- austenitne cevi

Abstract

This work uses computational thermomechanical model-based finite element analysis (FEA) to explore the effects of welding sequences on residual stresses that accumulate in the material and distortions of welded components, which are a direct outcome of residual stresses, the material microstructures, material properties, and eventually the fracture toughness. The consequences of the welding process are evaluated in this study in an austenitic pipe butt weld.

Izvod

U ovom radu je korišćena računarska termomehanička analiza na bazi modela konačnim elementima (FEA) kako bi se istražili uticaji sekvenci zavarivanja na zaostale napone koji se pojavljuju u materijalu, i deformacije zavarenih delova, koje su direktna posledica zaostalih napona, mikrostrukture materijala, svojstva materijala, kao i žilavosti loma. Posledice postupka zavarivanja su utvrđene u ovom radu kod spoja austenitnih cevi.

INTRODUCTION

Welding creates substantial thermal stress gradients around joints as a result of localised heating and subsequent cooling. These may cause weld deformation or cracking which will reduce the component's lifespan and functionality. As discussed by Withers et al. /1, 2/, this transient temperature field can make welded structures susceptible to hydrogen embrittlement and other negative occurrences. Understanding temperature evolution is essential, especially in high-integrity steel components, because the application of the heat source causes microstructural changes that could lead to a loss of structural integrity.

It is difficult to simulate any welding process using finite elements (FE) because of the interaction of thermal, mechanical, and metallurgical processes, /3-5/. Hibbitt et al. /6/ used a highly focused heat source in motion to address a heat transfer issue when conducting a thermal evaluation of a welding operation. One of the most widely used heat source models in welding analysis is the moving double ellipsoidal heat source model, created by Goldak et al. /7/. One of its advantages is that it can withstand a variety of fusion welding procedures. Due to the highly concentrated heat source, mesh refinement is required along the entire welding route, which increases the computational cost of welding analysis using FEA.

In the current research, appropriate finite element predictions are made using stainless steel (AISI-304). FEA utilizes temperature-dependent material properties sourced from /8/ for both the weld material and heat-affected zone. It is assumed that the material is homogenous and isotropic. Since a temperature range from room temperature to the material's melting point and above is experienced during welding, the temperature dependency of the material is fully accounted for, and the prescription of temperature-independent properties causes significant errors in the predicted results, /9/.

MATHEMATICAL MODEL

A moving heat source is a type of heat transfer phenomenon that can be applied to a variety of technical tasks, including welding. By figuring out the temperature distribution and cooling rate utilising theoretical solutions to this problem, engineers may be able to better understand the impacts of heat input and the performance of the finished product. These solutions have applications in welding for determining the microstructure, joint strength, residual stresses, cold cracking, size of heat-affected zone (HAZ), and deformation. The equations below state the double ellipsoid heat source model that best describes the heat source for arc welding:
- for the front heat source:

$$Q(x',y',z',t)=\frac{6\sqrt{3}f_f Q_w}{a_f bc\pi\sqrt{\pi}}e^{-3x'^2/a_f^2}e^{-3y'^2/b^2}e^{-3z'^2/c^2}, \quad (1)$$

- for the rear heat source:

$$Q(x',y',z',t)=\frac{6\sqrt{3}f_r Q_w}{a_r bc\pi\sqrt{\pi}}e^{-3x'^2/a_r^2}e^{-3y'^2/b^2}e^{-3z'^2/c^2}, \quad (2)$$

where: x, y, and z are the welded pipe's local coordinates; f_f and f_r are parameters that indicate the proportion of heat deposited in the front and rear portions, respectively. Note

that $f_f + f_r = 2.0$. The welding heat source's power is Q_w. Calculations can be made based on the welding current, arc voltage, and arc efficiency. It is assumed that the TIG welding technique has an arc efficiency η of 80 %.

Affecting the characteristics of the welding heat source are parameters a_f, a_r, b, and c. Under the welding requirements, the heat source's specifications can be changed to produce the necessary melted zone. The most efficient way to simulate arc operations is to use the approach in Fig. 1.

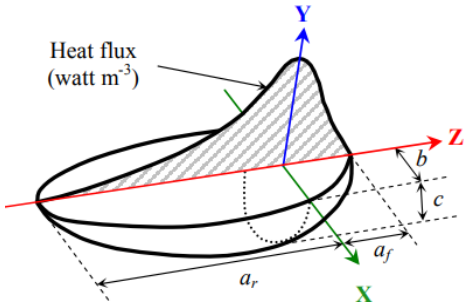

Figure 1. Heat source geometry, /6/.

Parameters for the welding process and the heat source are displayed in Tables 1 and 2, respectively.

Table 1. Parameters of the welding process

Parameters	Value
Welding voltage, (V)	12.5
Welding current, (A)	200
Welding speed, v (mm.s^{-1})	3
Welding process efficiency, η (%)	80

Table 2. Goldak heat source specifications.

Parameters	Value
Length of front ellipsoidal, a_f (mm)	2
Length of rear ellipsoidal, a_r (mm)	5
Width of heat source, 2b (mm)	6.6
Depth of heat source, c (mm)	5
Fraction of heat in front ellipsoidal, f_f	1.25
Fraction of heat in rear ellipsoidal, f_r	0.75

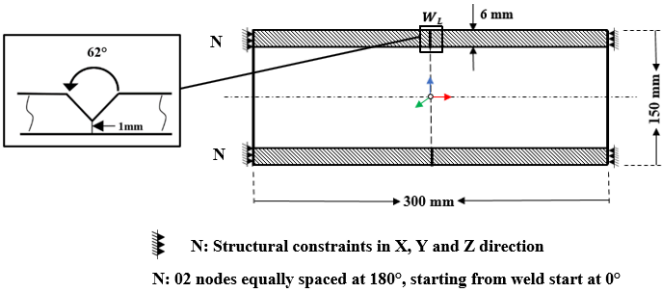

Figure 2. Graphic representations of geometric parameters and structural boundary conditions.

In Figure 3, boundary conditions for welding simulations naturally include both heat and mechanical factors. Free convection and radiation from the material are typically a part of the solution's thermal component. Mechanical boundary conditions are necessary for accurate deformation and stress prediction (Fig. 2). Studies that altered the mechanical boundary conditions and discovered noticeably varied material responses have been published, /10/.

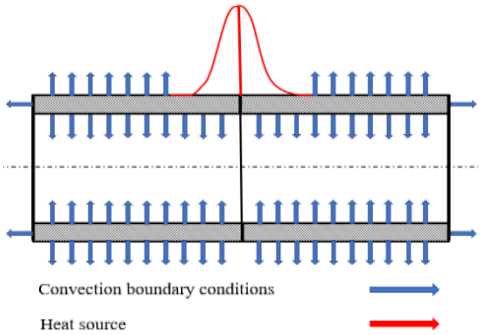

Figure 3. Schematic representations of thermal boundary conditions.

RESULTS

Figure 4 illustrates the multi-pass (4 layers) used in a wall thickness of 6 mm. A multi-pass welding process enables the welding of a wide range of weld joints of varying thicknesses. The FE application has recently grown in popularity within the industry. One of the newest FE programmes currently available is Simufact-Welding™. For the analysis and improvement of welding processes, it is a specially designed software programme.

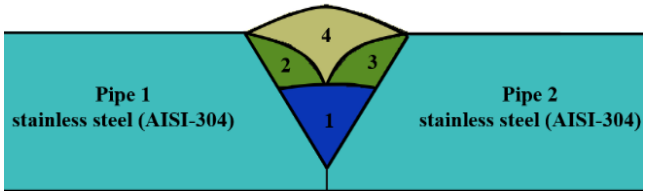

Figure 4. Vicinity of the multi-pass welding in a butt joint.

Many scientists have used commercial software to extensively predict the distortion caused by the heat of robotic welding. FEA is currently the preferred tool for welding simulation. After the completion of the welding simulation, the mechanical, thermal, and total distortion results are discussed in the following sections.

Temperature distribution

Thus, being able to forecast transient temperature fields is essential because it allows us to determine whether safety-critical welded components will be able to function in a satisfactory manner for the duration of their intended service.

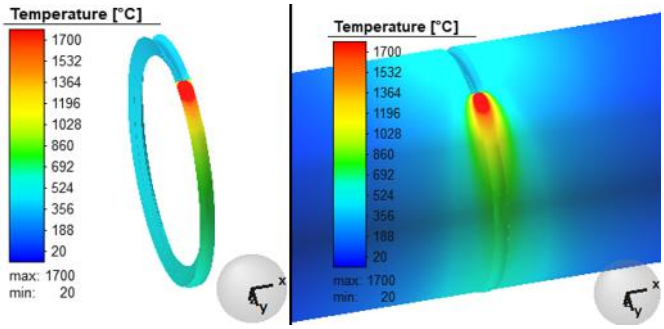

Figure 5. Temperature change in Robot and complete model, (°C).

Temperature change in Robot, the complete model, and the peak temperature at process time 328 s are presented in Figs. 5-6. Figure 7 presents the axial temperature distribution at 90° from weld start.

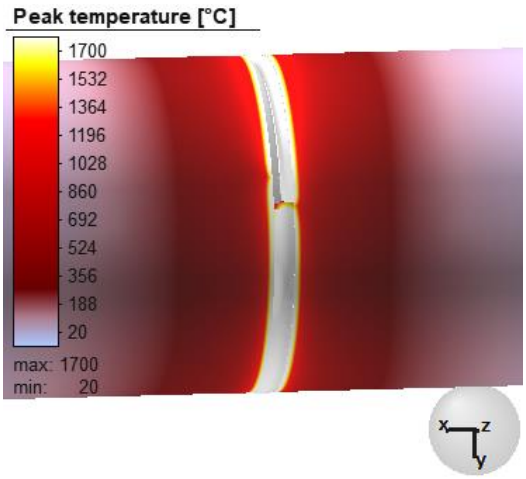

Figure 6. Peak temperature change, (°C).

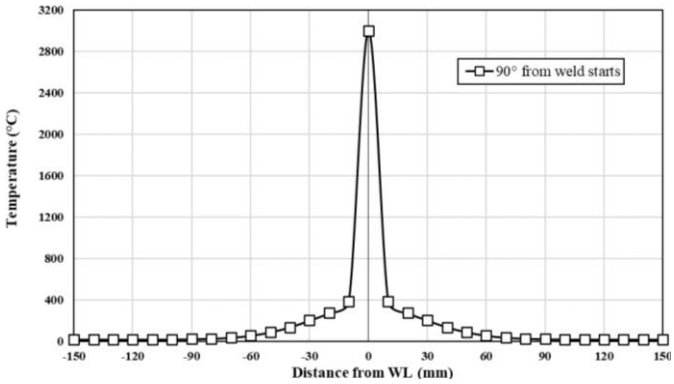

Figure 7. Axial temperature distribution at 90° from weld start, (C°).

Angular distortion

In order to fuse the materials together during welding, the joint is typically heated. Expansion and contraction appear from this heat. Distortion may occur if heating and cooling are unequal. The residual stress is what causes this deformation. Only the change in weld area volume and subsequent movement of the material after it hardens and cools to room temperature can be used to determine the extent of thermal stress applied to the material, and Figs. 8-9 confirm that.

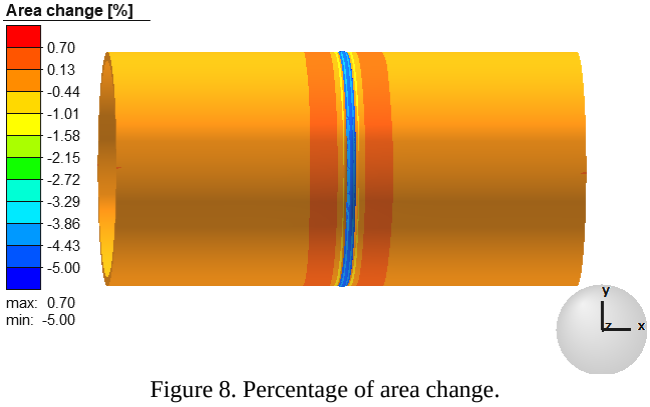

Figure 8. Percentage of area change.

When the angles between the welded components change by contraction, angular distortion occurs. Due to the larger weld pool at the top than at the bottom, the contraction is more noticeable, as shown in Fig. 10.

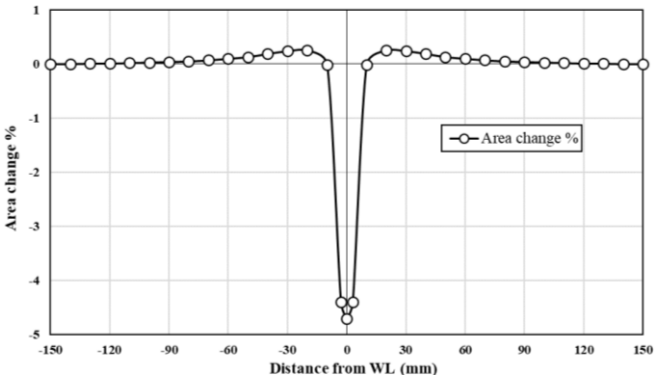

Figure 9. Axial distortion, (%).

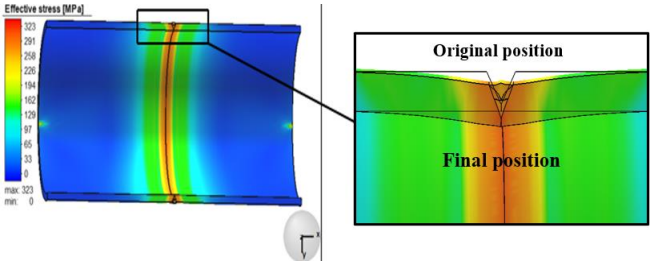

Figure 10. Effective stress change, (MPa).

Residual stress

Residual stresses in welded joints primarily developed due to differential heating, peak temperature, and cooling at any moment during welding. As shown in Fig. 10, the amount of residual stress after welding simulation shows vast differences.

On the outer and inner surfaces of the cylinders, the compressive and tensile axial stress fields, respectively, are shown in, and are close to the weld zone. This is explained by the differing temperature profiles on the cylinders' inner and outer surfaces. Tensile and compressive residual stress fields are produced on inner and outer surfaces, respectively, along the weld line, as a result of varying shrinkage patterns through the wall thickness, caused by distinct temperature gradients (WL), as shown in Figs. 11-12.

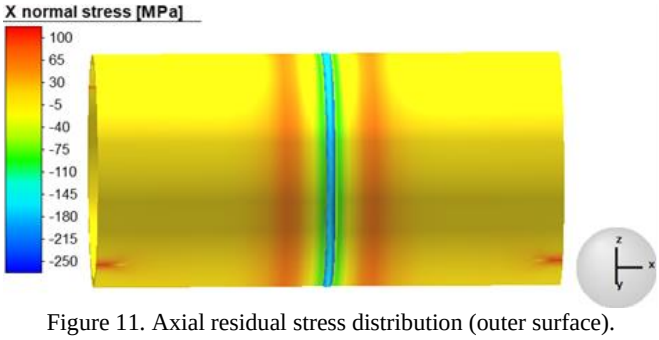

Figure 11. Axial residual stress distribution (outer surface).

Axial stress distributions on the outer and inner surface of the cylinders at various cross-sections from the weld start location are shown in Figs. 13-14.

By referring to Fig. 13, high compressive stresses appear near the WL. After 14 mm on each side of the WL, the compressive residual axial stresses near the WL vanish to zero. Beyond this, the stress character is found to switch from compressive to tensile. Nearly 70 mm distant from the WL, these low-magnitude tensile stresses once more approach a zero value.

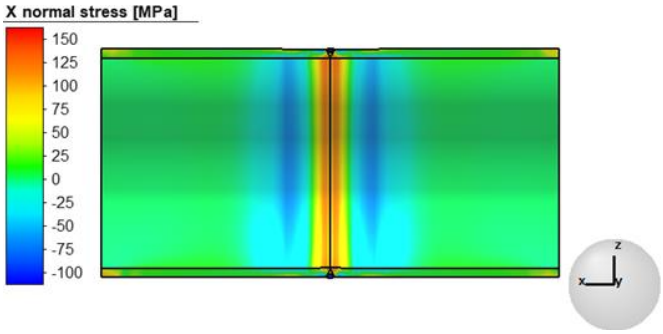

Figure 12. Axial residual stress plots on the inner surface.

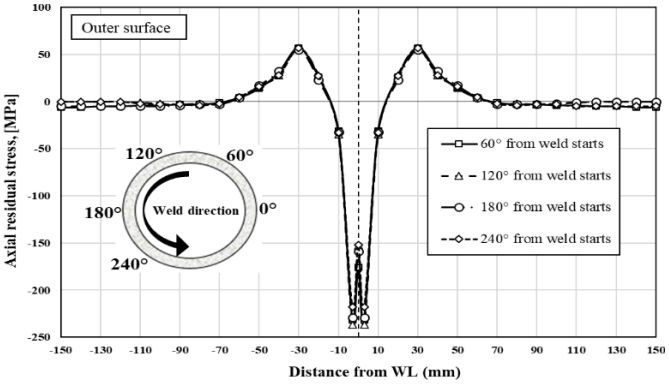

Figure 13. Axial residual stress plots on the outer surface.

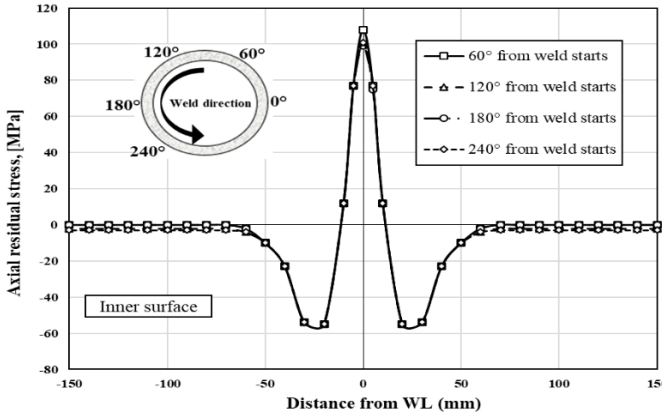

Figure 14. Axial residual stress distribution (inner surface).

For inner surfaces of the cylinder at various cross sections from the weld start position, the high tensile stresses near the WL approach zero and then reverse to lower compressive residual stresses at 14 mm, increasing to an almost constant value of zero at 70 mm, as shown in Fig. 14.

The position around the circumference has only a minimal influence on axial stresses. Axial residual stresses on the outer and inner surfaces for four different cross sections (60°, 120°, 180°, and 240°) are virtually of the same magnitude and trend, as shown in Figs. 13 and 14.

CONCLUSIONS

The following conclusions are reached based on the total distortion and residual stresses in austenitic pipe butt joints:

– the results of the welding simulation show that the yield strength of the material was not considerably influenced by the total distortion that occurred at the multi-pass weld on the tubular butt joint and indicates that the weld metal has greater residual stress in comparison to other structural components;
– there is a significant axial residual stress along and around the weld line, as well as on the inner and outer surfaces of the pipe, respectively. On the inner and outer surfaces distant from the weld line, axial residual stresses are produced. These stresses can be compressive or tensile;
– a multi-pass weld can increase joint strength, weld greater thicknesses, and temper the previously deposited weld (resulting in a microstructure with less residual stress).

ACKNOWLEDGMENTS

The authors acknowledge the Ministry of Higher Education and Scientific Research ‘Ministère de l’Enseignement Supérieur et de la Recherche Scientifique (MESRS)’, Algeria, for technical and financial support (Project code A01L 09UN410120200002).

REFERENCES

1. Withers, P.J., Bhadeshia, H.K.D.H. (2001), *Residual stress. Part 1 - Measurement techniques*, Mater. Sci. Technol. 17(4): 355-365. doi: 10.1179/026708301101509980
2. Withers, P.J., Bhadeshia, H.K.D.H. (2001), *Residual stress. Part 2 - Nature and origins*, Mater. Sci. Technol. 17(4): 366-375. doi: 10.1179/026708301101510087
3. Tsirkas, SA., Papanikos, P., Kermandis, Th. (2003), *Numerical simulation of the laser welding process in butt-joint specimens*, J Mater. Process. Technol. 134(1): 59-69. doi: 10.1016/S0924-0136(02)00921-4
4. Perret, W., *Welding simulation of complex automotive welded assembly - Possibilities and limits of the application of analytical temperature field solutions*, Ph.D. Thesis, Technischen Universität Berlin, Fakultät V - Verkehrs- und Maschinensysteme ISBN 3981594401 BAM, 2013, p.184.
5. Perret, W., Schwenk, C., Ethmeier, M.R., et al. (2011), *Case study for welding simulation in the automotive industry*, Weld. in the World, 55: 89-98. doi: 10.1007/BF03321546
6. Hibbitt, H.D., Marcal, P.V. (1973), *A numerical, thermo-mechanical model for the welding and subsequent loading of a fabricated structure*, Comput. Struct. 3(5): 1145-1174. doi: 10.1016/0045-7949(73)90043-6
7. Goldak, J., Chakravarti, A., Bibby, M. (1984), *A new finite element model for welding heat sources*, Metall. Trans. B, 15: 229-305. doi: 10.1007/BF02667333
8. Zeghida, C., Belyamna, M.A., Tlili, S., Guedri, A. (2022), *The effect of induction heating stress remedies on piping reliability*, Procedia Struct. Integ. 41: 384-393. doi: 10.1016/j.prostr.2022.05.044
9. Lindgren, L.E. (2001), *Finite element modeling and simulation of welding. Part 2: Improved material modeling*, J Therm. Stresses, 24(3): 195-231. doi: 10.1080/014957301300006380
10. Bae, K.-Y., Na, S.-J. (1995), *A study of the effect of pre-straining on angular distortion in one-pass fillet welding incorporating large deformation theory*, Proc. Inst. Mech. Eng., Part B: J Eng. Manuf. 209(5): 401-409. doi: 10.1243/PIME_PROC_1995_209_099_02